

Role of the transition metal in Grignard metathesis polymerization (GRIM) of 3-hexylthiophene†

Cite this: *J. Mater. Chem. A*, 2013, **1**, 12841Mahesh P. Bhatt,^a Harsha D. Magurudeniya,^a Prakash Sista,^a Elena E. Sheina,^b Malika Jeffries-EL,^c Benjamin G. Janesko,^{*d} Richard D. McCullough^e and Mihaela C. Stefan^{*a}

Regioregular poly(3-alkylthiophene)s are widely used in organic electronics applications such as solar cells and field effect transistors. Nickel, palladium, and platinum diphenylphosphinoethane complexes were tested as catalysts for the Grignard metathesis (GRIM) polymerization of 2,5-dibromo-3-hexylthiophene and 2-bromo-5-iodo-3-hexylthiophene. Nickel-mediated polymerization generated regioregular, low-polydispersity poly(3-hexylthiophene) with well-defined molecular weight consistent with a “living” chain-growth mechanism. By contrast, palladium-mediated polymerization proceeded by a step-growth mechanism and generated polymers with less than 80% head-to-tail couplings. Platinum-mediated polymerization gave very low molecular weight products. Kinetic and computational results suggested that the nickel catalyst acts as an initiator and remains associated with the growing polymer chain, while palladium dissociates from the growing chain. Computational and experimental evidence was provided for various side reactions of dissociated Pd(0) catalyst, which could yield a step growth mechanism and lower regioirregularity.

Received 16th August 2013
Accepted 6th September 2013

DOI: 10.1039/c3ta13258g

www.rsc.org/MaterialsA

Introduction

Poly(3-alkylthiophene)s are the most used semiconducting polymers for organic electronics applications.^{1,2} The asymmetric 3-alkyl-2,5-dihalothiophene monomer can generate multiple intra-monomer orientations: “head-head”, “head-tail”, and “tail-tail”. Regioregular polymers containing almost exclusively head-to-tail couplings have improved opto-electronic properties as compared to the regioirregular analogues.³ Synthesis of regioregular poly(3-hexylthiophene) (P3HT) utilizing either Kumada or Negishi metal-mediated cross-coupling reactions were first reported in 1992.^{4–10} Both methods require cryogenic temperatures to generate regioregular polymer. The Grignard metathesis (GRIM) polymerizations was reported by McCullough's group in 1999 and allows the synthesis of regioregular P3HT in large scale without the use of cryogenic reaction

conditions.¹¹ Later, McCullough and Yokozawa reported the quasi-“living” nature of GRIM polymerization.^{11–14}

Scheme 1 shows the accepted mechanism for the nickel mediated GRIM polymerization. The cyclic chain growing reaction begins with a M(n)-halide complex bound to the growing chain end (7). The transition metal M is typically Ni. The nickel complex undergoes transmetalation with the 5-halomagnesium thiophene monomer (2). Reductive elimination then forms a new thiophene–thiophene bond. The remaining Ni(0)(dppe) complex is speculated to form an “associated pair” with the thiophene chain end. Subsequent oxidative addition to the terminal carbon–halogen bond regenerates the nickel complex.

McCullough and coworkers demonstrated that GRIM polymerization has some characteristics of a “living” chain growth polymerization. This “living” polymerization enabled the end-functionalization and generated polymers with well-defined molecular weights and relatively narrow polydispersity index.^{14–17} Yokozawa's group also reported the “living” behavior of nickel catalyzed cross-coupling polymerization of 2-bromo-5-iodo-3-hexylthiophene.^{13,17} Subsequent work by Luscombe, Kiriya, Locklin, and McNeil^{18–27} had provided additional experimental evidence for the presence of the associated pair between Ni(0) and the growing chain. Dissociation of free Ni(0) is presumed to yield various side reactions, possibly including inter-chain coupling, and non-“living” behavior.^{28–30}

We investigated the kinetics of GRIM polymerization of 2,5-dibromo-3-hexylthiophene (DBHT) and 2-bromo-5-iodo-3-hexylthiophene (IBHT) monomers with Ni(dppe)Cl₂, Pd(dppe)Cl₂,

^aUniversity of Texas at Dallas, Department of Chemistry, 800 West Campbell Road, Richardson, TX 75080, USA. E-mail: mihaela@utdallas.edu; Fax: +1 972-883-2925; Tel: +1 972-883-6581

^bPlextronics, Inc, 2180 WilliamPitt Way, Pittsburgh, PA 15238, USA. E-mail: ESheina@plextronics.com

^cIowa State University, Department of Chemistry, 3101C Hach Hall, Ames, IA 50011, USA. E-mail: malikaj@iastate.edu

^dTexas Christian University, Department of Chemistry, TCU Box 298860, Forth Worth, TX 76129, USA. E-mail: b.janesko@tcu.edu

^eHarvard University, 1350 Massachusetts Avenue, Holyoke Center, Suite 836, Cambridge, MA 02138, USA. E-mail: richard_mccullough@harvard.edu

† Electronic supplementary information (ESI) available: ¹H NMR spectra, kinetic plots, and SEC traces. See DOI: 10.1039/c3ta13258g



Structural analysis

^1H NMR spectra of the P3HT polymers were recorded on a Bruker-500 MHz spectrometer at room temperature. ^1H NMR data are reported in parts per million as chemical shift relative to tetramethylsilane (TMS) as the internal standard. Spectra were recorded in CDCl_3 . GC/MS was performed on an Agilent 6890-5973 GC-MS workstation. The GC column was a Hewlett-Packard fused silica capillary column cross-linked with 5% phenylmethyl siloxane. Helium was the carrier gas (1 mL min^{-1}). The following conditions were used for all GC/MS analyses: injector and detector temperature, $250 \text{ }^\circ\text{C}$; initial temperature, $70 \text{ }^\circ\text{C}$; temperature ramp, $10 \text{ }^\circ\text{C min}^{-1}$; final temperature, $280 \text{ }^\circ\text{C}$.

Molecular weights of the synthesized polymers were measured by Size Exclusion Chromatography (SEC) analysis on a Viscotek VE 3580 system equipped with Viscogel™ columns (GMHHR-M), connected to a refractive index (RI) detectors. GPC solvent/sample module (GPCmax) was used with HPLC grade THF as the eluent and calibration was based on polystyrene standards. Running conditions for SEC analysis were: flow rate = 1.0 mL min^{-1} , injector volume = $100 \mu\text{L}$, detector temperature = $30 \text{ }^\circ\text{C}$, column temperature = $35 \text{ }^\circ\text{C}$. All the polymers samples were dissolved in THF and the solutions were filtered through PTFE filters ($0.45 \mu\text{m}$) prior to injection.

Polymerization experiment

In a typical experiment, a dry 100 mL three-neck round bottom flask was connected to a nitrogen line and charged with 2,5-dibromo-3-hexylthiophene (1.6 g, 5.0 mmol), *p*-dimethoxybenzene (internal standard) (0.2 g), and anhydrous THF (10 mL). A 2 M solution of alkyl magnesium chloride (2.5 mL, 5.0 mmol) in diethyl ether (Et_2O) was added *via* a deoxygenated syringe, and the reaction mixture was reacted at room temperature for 2 hours. At this time an aliquot (0.5 mL) was taken out and quenched with water. The organic phase was extracted in Et_2O and subjected to GC-MS analysis to determine the composition of the reaction mixture. The main components of the reaction mixture were 2-bromo-5-chloromagnesium-3-hexylthiophene and 5-bromo-2-chloromagnesium-3-hexylthiophene regioisomers. Usually less than 5% of unreacted 2,5-dibromo-3-hexylthiophene was detected by GC-MS analysis. The concentration of 2-bromo-5-chloromagnesium-3-hexylthiophene isomer was estimated to 80 mol%. Before the addition of the catalyst, 40 mL of anhydrous THF was added to the reaction mixture, followed by the addition $\text{Ni}(\text{dppe})\text{Cl}_2$ (0.04 g, 0.075 mmol). After addition of $\text{Ni}(\text{dppe})\text{Cl}_2$, aliquots (1 mL) were taken at different time intervals and each was precipitated in methanol (5 mL). For each aliquot a sample was prepared in Et_2O (2 mL) and subjected to GC-MS analysis for the determination of concentration of unreacted monomer. After filtration through PTFE filters ($0.45 \mu\text{m}$), the molecular weight of the polymer samples was measured by SEC with THF as the eluent. Polymerization of 2-bromo-5-iodo-3-hexylthiophene was performed in a similar manner.

Chain scissoring experiment

In a 100 mL two neck flask $\text{Pd}(\text{dppe})\text{Cl}_2$ (10 mg, 0.01 mmol) was dispersed in 10 mL of THF under a nitrogen atmosphere. Sodium metal (1 g, 43 mmol) was added to the reaction mixture and was stirred for 5 hours. At this point, the color of the reaction mixture turned to yellowish green which is due to the formation of Pd(0). A solution of poly(3-hexylthiophene), (100 mg, 0.0025 mmol, $M_n = 38\,000 \text{ g mol}^{-1}$), was prepared in 100 mL of freshly distilled THF. The Pd(0) catalyst was cannulated into the solution of P3HT. Magnesium bromide (10 mg, 0.05 mmol) was added to the reaction flask and the reaction mixture was stirred for 12 hours under a nitrogen atmosphere. The reaction was quenched with methanol and the polymer was filtered and purified by using Soxhlet extractions with methanol, hexane and chloroform. No polymer was collected from the methanol and hexane fractions. All the polymer was collected from the chloroform fraction.

Computations

All calculations used the Gaussian 09 electronic structure package.³² Unless noted otherwise, calculations used density functional theory with the M06 exchange–correlation functional,³³ the LANL08 basis set and relativistic effective core potential on Ni, Pd, and Pt;^{34,35} and the 6-31+G(d,p) basis set on all other atoms.^{36,37} Geometries and free energy corrections are evaluated with the PBE0 hybrid exchange–correlation functional and the LANL2DZ basis set and core potential. M06 self-consistent field calculations use Gaussian keyword “SCF = Tight”, and use a numerical integration grid with 99 radial and 590 angular points per atom (Gaussian keyword “Integral(Grid = UltraFine)”).

Results and discussion

A magnesium halogen exchange reaction between DBHT and *t*-butylmagnesium chloride generated regioisomers (2) and (3) (Scheme 1) in a ratio of 80 to 20, as determined by GC-MS analysis. Initially, $\text{Ni}(\text{dppe})\text{Cl}_2$ was used as a catalyst and the kinetics of polymerization was monitored. GC-MS analysis of the quenched reaction mixture, after the addition of $\text{Ni}(\text{dppe})\text{Cl}_2$ indicated that only monomer (2) was consumed during polymerization. Isomer (3) was not consumed during the nickel-mediated polymerization. The monomer conversion for the $\text{Ni}(\text{dppe})\text{Cl}_2$ catalyzed reaction was thus calculated from the consumption of isomer (2). The conversion *vs.* time plot (Fig. 1B, top) shows that the polymerization was fast, reaching 98% conversion in 10 minutes. The molecular weight *vs.* conversion plot (Fig. 1B, bottom) shows a linear increase of molecular weight with conversion. This is consistent with previous reported data which demonstrated the quasi-“living” nature of GRIM polymerization of DBHT with $\text{Ni}(\text{dppp})\text{Cl}_2$ initiator.¹⁴ The polydispersity index of the collected polymer samples has a value of ~ 1.23 (the polydispersity index *vs.* conversion plots is shown in the ESI†).



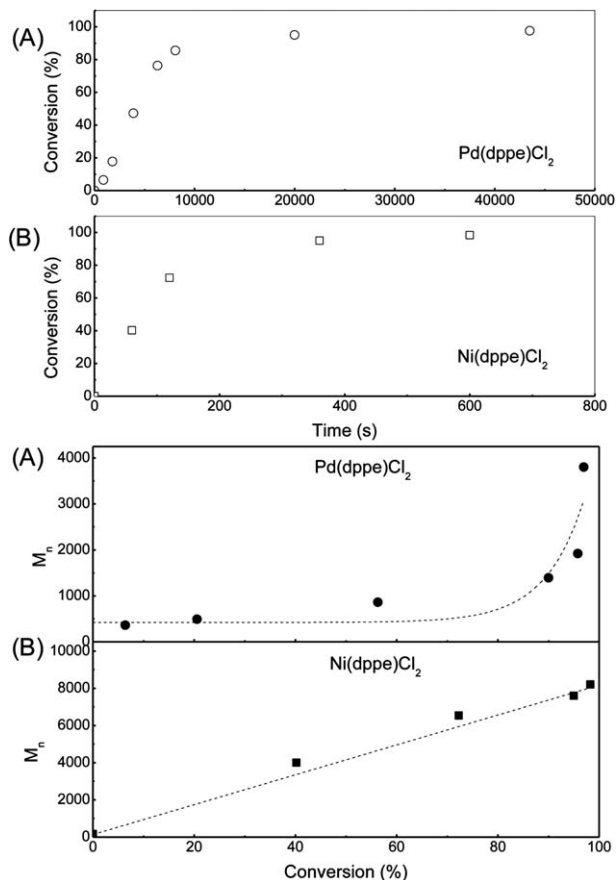


Fig. 1 Conversion vs. time (top) and number average molecular weight vs. conversion (bottom) plots for GRIM polymerization of 2,5-dibromo-3-hexylthiophene. (A) [DBHT]₀ = 0.1 mol L⁻¹; [Pd(dppe)Cl₂]₀ = 0.0015 mol L⁻¹; temp = 45 °C. (B) [DBHT]₀ = 0.1 mol L⁻¹; [Ni(dppe)Cl₂]₀ = 0.0015 mol L⁻¹; temp = 23 °C.

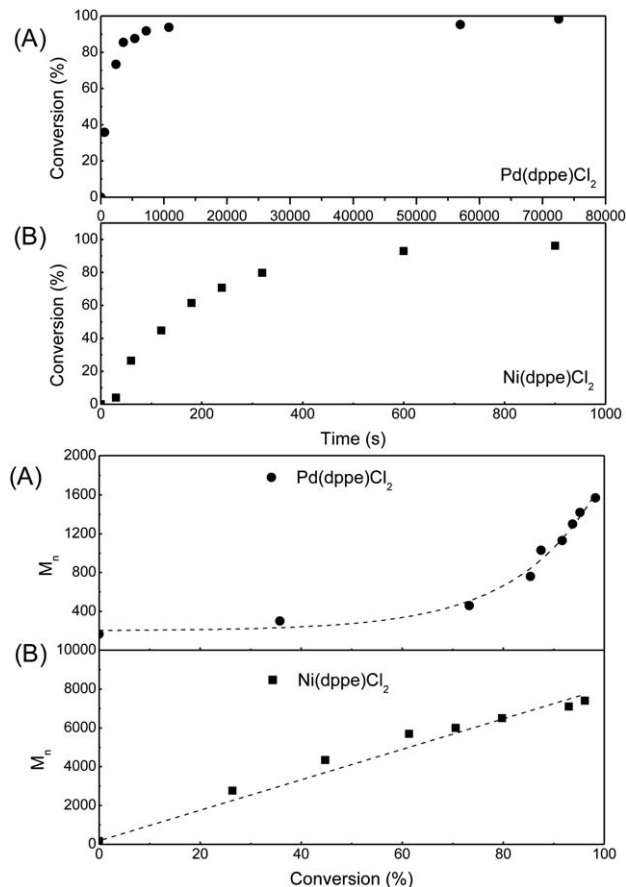


Fig. 2 Conversion vs. time (top) and number average molecular weight vs. conversion (bottom) plots for GRIM polymerization of 2-bromo-5-iodo-3-hexylthiophene. (A) [IBHT]₀ = 0.1 mol L⁻¹; [Pd(dppe)Cl₂]₀ = 0.0015 mol L⁻¹; temp = 45 °C. (B) [IBHT]₀ = 0.1 mol L⁻¹; [Ni(dppe)Cl₂]₀ = 0.0015 mol L⁻¹; temp = 23 °C.

GRIM polymerization of DBHT was also performed with Pd(dppe)Cl₂ catalyst. Polymerization under the above conditions was very slow, reaching less than 30% conversion in 24 h. To increase the rate of polymerization, the reaction with Pd(dppe)Cl₂ catalyst was performed at 45 °C. The conversion vs. time plot (Fig. 1A, top) showed that, even at this elevated temperature, 98% monomer conversion required 12 hours of polymerization time. In a remarkable contrast to the nickel-mediated reaction, polymerization with Pd(dppe)Cl₂ catalyst consumed both isomers (2) and (3). (Conversion vs. time plots for isomers (2) and (3) are shown in ESI†).

The observed non-linear dependence of the molecular weight as a function of conversion resembles the behavior of a step-growth polymerization (Fig. 1A, bottom). GRIM polymerization of DBHT was also performed with Pt(dppe)Cl₂ catalyst. This polymerization was very slow, reaching only 80% conversion in 48 h at 45 °C and producing only dimer and small oligomers ($M_n = 800 \text{ g mol}^{-1}$). GC-MS analysis of the reaction mixture indicated the presence of the 5,5'-dibromo-4,4'-dihexyl-2,2'-bithiophene dimer intermediate (6). This is consistent with the fact that, to our knowledge, platinum catalysts have not been successfully used for Kumada cross-coupling.^{38–45}

The polymerization experiments were repeated with IBHT monomer. This monomer is known to form only one regioisomer (2), which was expected to lead to the formation of regioregular P3HT. The observed reaction rates are comparable to those for DBHT (Fig. 2, top). Molecular weight vs. conversion plots also show the same trends as observed for DBHT polymerization, with the Ni(dppe)Cl₂ and Pd(dppe)Cl₂ catalysts respectively displaying linear and non-linear dependence of molecular weight with conversion (Fig. 2, bottom). As for DBHT, the Pt(dppe)Cl₂ catalyst gave very slow polymerization yielding only dimer and small oligomers. The polydispersity index vs. conversion plots for IBHT polymerizations are included in the ESI.†

Computational investigations

The previously reported paper by McCullough suggested that the “associated pair” (9) is critical to the chain-growth mechanism of GRIM.¹⁴

Based on this prior report, we hypothesized that the high polydispersity and regioirregularity observed for Pd(dppe) catalyst was due to side reactions of free Pd(0), which could be produced by dissociation of the associated pair. (Note that the



accepted mechanism of Scheme 1 does not contain free zero-valent metal.) We further speculate that the very slow Pt-catalyzed polymerization is due to “poisoning” by thiophene.

First, we examined the potential energy surface for the $M(0)$ [1,2-bis(dimethylphosphino) ethane (dmpe)]-thiophene associated pair to undergo either oxidative insertion into the chain end, or dissociation off of the growing chain. Fig. 3 shows the calculated potential energy surfaces for $M = (\text{Ni}, \text{Pd}, \text{Pt})$, with the zero of free energy set to the associated pair. The three metals give roughly comparable free energy differences and barriers for oxidative addition. However, $M = \text{Pd}$ had a much smaller free energy of dissociation. Counterpoise corrected calculations give similar trends, with dissociation free energies of $32.9 \text{ kcal mol}^{-1}$ for Ni, $8.3 \text{ kcal mol}^{-1}$ for Pd, and $22.7 \text{ kcal mol}^{-1}$ for Pt. These calculations are unlikely to reproduce the experimental binding free energies, due to limitations of the solvent model, an ideal gas model for translational and rotational free energies, and so on. However, the trends for different metals may reasonably be expected to be qualitatively correct. This suggested that the Pd associated pair is much less stable than Ni or Pt. The calculated total energy for dissociation of the associated pair between Ni(dmpe) and 2-bromo-3-methyl-5-(3-methylthiophenyl) thiophene is $48.8 \text{ kcal mol}^{-1}$, vs. $47.2 \text{ kcal mol}^{-1}$ for the system in Fig. 3. The calculated oxidative addition barrier for this dithiophene model is $12.3 \text{ kcal mol}^{-1}$, vs. $11.8 \text{ kcal mol}^{-1}$ for the system in Fig. 3. It is worth noting that dissociation of the associated pair (9) would yield a di-bromo-terminated thiophene chain. This is in line with the experimental studies, showing that “living” Grignard

metathesis yields a high proportion of (H/Br)-terminated chains.¹⁴

Next, we explored one possible mechanism for step-growth kinetics, oxidative addition of free $\text{Pd}(0)(\text{dmpe})$ to monomer. Fig. 4 compares the PBE0/LANL2DZ free energy surfaces for $\text{Pd}(0)(\text{dmpe})$ oxidative addition to the growing chain (modeled as in Fig. 3 as 2-bromo-3-methylthiophene) vs. Monomer 2 (modeled as 2-bromo-3-methyl-5-magnesiochloro thiophene). The potential energy surfaces are almost identical, indicating that free $\text{Pd}(0)$ is as likely to react with monomer as with the growing chain. M06 calculations give qualitatively similar results, with oxidative addition barriers of $13.1 \text{ kcal mol}^{-1}$ for the growing chain and $12.9 \text{ kcal mol}^{-1}$ for the monomer. Transmetalation of this oxidative addition product could yield multiple thiophene chains per Pd and subsequently step-growth kinetics.

Similar results were found for $\text{Ni}(0)(\text{dppe})$. Relative to the associated pair, the PBE0/LANL2DZ total energy barriers to $\text{Ni}(0)$ oxidative addition are $11.8 \text{ kcal mol}^{-1}$ for 2-bromo-3-methylthiophene, $12.3 \text{ kcal mol}^{-1}$ for 2-bromo-3-methyl-5-(3-methylthiophenyl) thiophene, $11.6 \text{ kcal mol}^{-1}$ for 2-bromo-3-methyl-5-magnesiochloro thiophene (equivalent to monomer 2 in Scheme 1), and only $10.0 \text{ kcal mol}^{-1}$ for 2-bromo-4-methyl-5-magnesiochloro thiophene (equivalent to monomer 3 in Scheme 1). Next, we explored whether free $\text{Pd}(0)(\text{dmpe})$ could produce regioregular polymer.

Here it is critical to recall that $\text{Pd}(\text{dppeCl}_2)$ catalyzed polymerization of IBHT, which only used monomer [2], still yielded regioregular polymer. We suggest one possible mechanism for

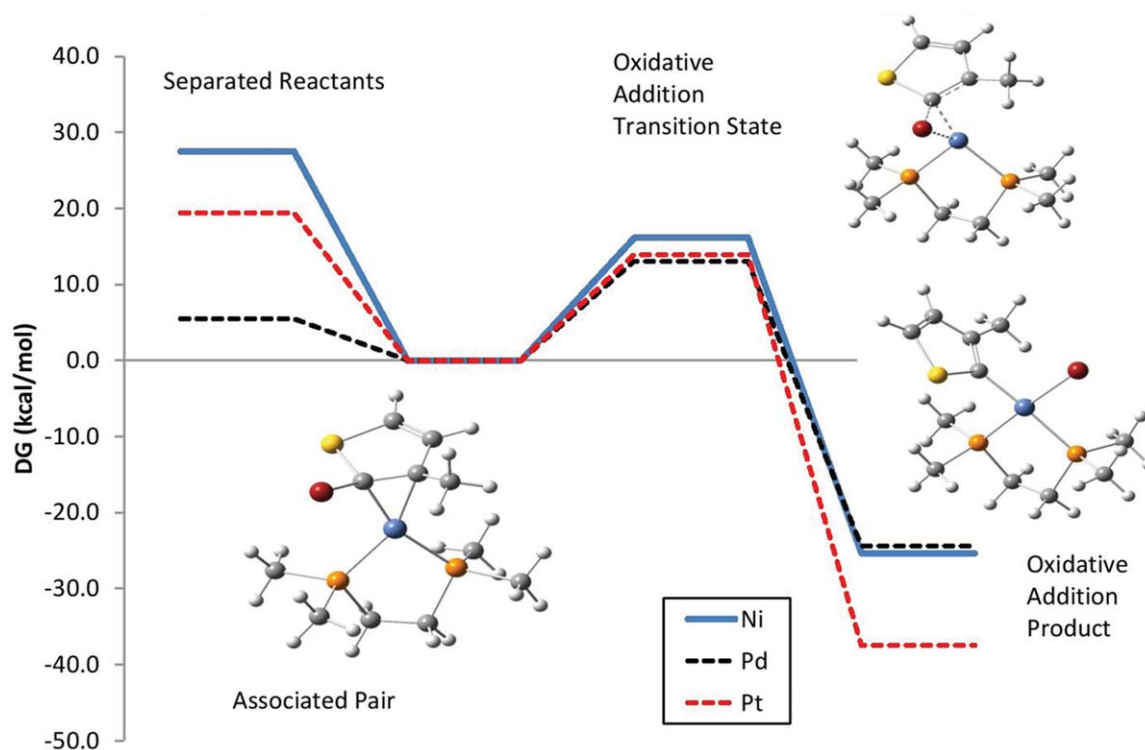


Fig. 3 Calculated free energy surface for the associated pair between $M(\text{dmpe})$ and a 2-bromo-3-methylthiophene model for the growing chain to undergo dissociation (left) or oxidative addition (right). Calculated geometries for $M = \text{Ni}$ are shown for each species.



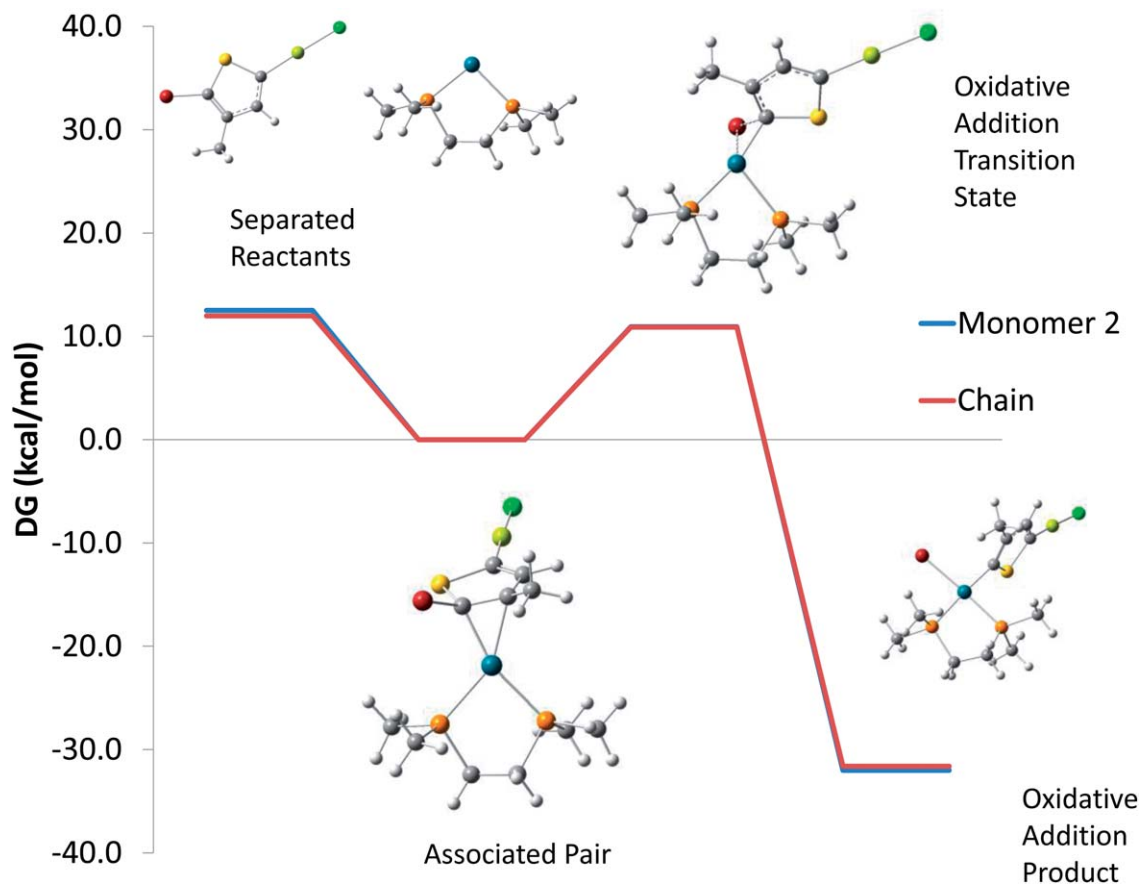
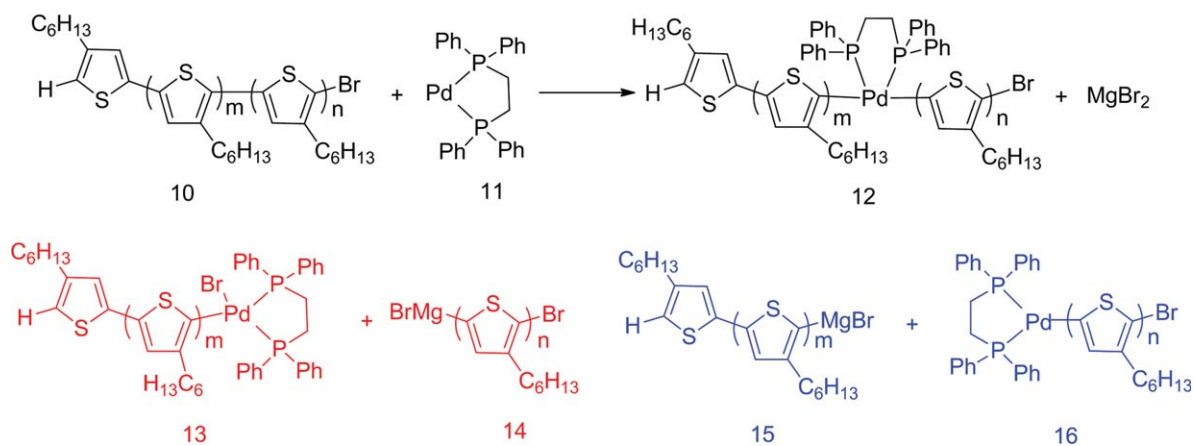


Fig. 4 Calculated free energy surface for the associated pair between Pd(dmpe) and either 2-bromo-3-methyl-5-magnesioclho thiophene monomer or a 2-bromo-3-methylthiophene model for the growing chain to undergo dissociation (left) or oxidative addition (right). Calculated geometries for the monomer case are shown for each species.

this in Scheme 2. In this mechanism, the free Pd(0)(dppe) discussed above inserts into the middle of regioregular polymer chain [10] (Scheme 2), which could be considered the equivalent of the reverse of reaction 8 → 9 from Scheme 1. The product undergoes transmetalation with free MgBr₂ (Scheme 2) which is

the equivalent of the reverse of reaction 7 → 8 from Scheme 1. This transmetalation could produce two possible products depending on which of the two chains is displaced from Pd. Products [13] and [14] (Scheme 2) would produce regioregular polymer, though the kinetics would likely not be chain-growth.



Scheme 2 Proposed chain scissoring mechanism in Pd(dppe)Cl₂ catalyzed polymerization of 3-hexylthiophene.



In contrast, transmetalation of product [16] (Scheme 2) with monomer [2] (Scheme 1) would generate a second TT defect, and transmetalation of product [15] (Scheme 2) with growing chain [7] (Scheme 1) would introduce a HH defect.

To test whether the back-reaction of Scheme 2 is feasible, we calculated the free energy surface for transmetalation of [7] (which is the equivalent of the oxidative addition product of Fig. 2) with monomer [2] (Scheme 1), and subsequent reductive elimination to the associated pair [9] (Scheme 1). These calculations use Ni(dmpe), preliminary results suggest comparable values for Pd(dmpe). Fig. 5 shows the PBE0/LANL2DZ free energy surface. M06 calculations give qualitatively similar results. The reactant [7 + 2] and product [9] + MgClBr have comparable free energies. The largest free energy barrier was found for the forward direction, and encompasses the loss of MgClBr from the transmetalation product and subsequent reductive elimination.

This suggests that the reactions $7 \rightarrow 8 \rightarrow 9$ and $9 \rightarrow 8 \rightarrow 7$ are comparably favorable.

To test whether the proposed chain scissoring for the Pd catalyzed polymerization was possible we performed an experiment using a regioregular P3HT polymer of a known molecular weight ($M_n = 38\,000\text{ g mol}^{-1}$, PDI = 1.36). The P3HT polymer used in this study was synthesized by GRIM method using Ni(dppp)Cl₂ as a catalyst. The ¹H NMR spectrum of the P3HT showed 66% of H/Br and 40% of H/H end groups before the chain scissoring

experiment. The polymer was dissolved in THF and reacted with Pd(0) for 12 hours. The Pd(0) complex was generated from the reduction of Pd(dppe)Cl₂ with sodium metal. The colour change from brown to green yellow was used as an indicative for the formation of Pd(0) complex. MgBr₂ was added to the reaction mixture containing P3HT and Pd(0) complex to facilitate the transmetalation as proposed in the mechanism shown in Scheme 2. The resulting polymer exhibited a lower molecular weight and a broader PDI as compared to the starting P3HT polymer (ESI†). The molecular weight of the resulting polymer was also reduced to $25\,000\text{ g mol}^{-1}$ from $38\,000\text{ g mol}^{-1}$ while the PDI broadened from 1.36 to 1.60. While it is difficult to predict at which position the scissoring is taking place, the decrease in the molecular weight of P3HT and the broadening of PDI can be reasonably considered as an indicative of the chain scissoring. Moreover, the ¹H NMR analysis indicated that the final polymer obtained after the chain scissoring experiment had only H/H end groups (see the ¹H NMR spectra in ESI†) which show the absence of a triplet at 2.6 ppm which is due to the hexyl methylene protons adjacent to the bromine end group.

Conclusions

In conclusion, we studied the mechanistic differences of group 10 transition metal-mediated GRIM polymerization for the synthesis of P3HT. The presented experimental evidence and

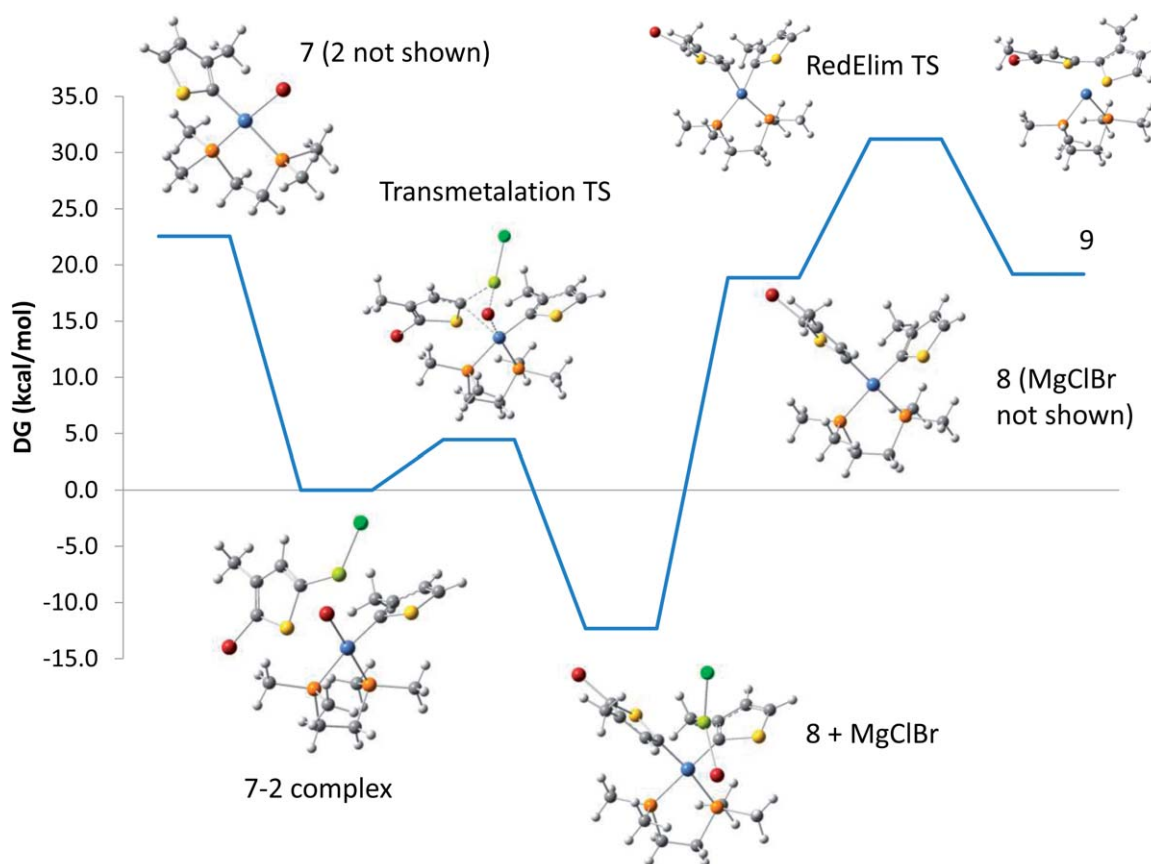


Fig. 5 Calculated free energy surface for reaction $7 \rightarrow 8 \rightarrow 9$ of Scheme 1, catalyzed by Ni(dmpe).



the proposed mechanisms bring additional support particularly for the presence of the associated pair of 5,5'-dibromo-4,4'-dihexyl-2,2'-bithiophene dimer and Ni(0) in the mechanism of Grignard metathesis (GRIM) polymerization.

Acknowledgements

Financial support for this project from NSF (Career DMR-0956116) and Welch Foundation (AT-1740) is gratefully acknowledged. We gratefully acknowledge the NSF-MRI grant (CHE-1126177) used to purchase the Bruker Avance III 500 NMR instrument.

Notes and references

- 1 T. A. Skotheim and J. Reynolds, *Handbook of Conducting Polymers*, CRC Press, LLC, Boca Raton, 2006.
- 2 *Handbook of Thiophene-Based Materials: Applications in Organic Electronics and Photonics, Volume One: Synthesis and Theory*, ed. I. F. Perepichka and D. F. Perepichka, 2009.
- 3 R. D. McCullough, *Adv. Mater.*, 1998, **10**, 93–116.
- 4 R. D. McCullough and R. D. Lowe, *J. Chem. Soc., Chem. Commun.*, 1992, 70–72.
- 5 R. D. McCullough, R. D. Lowe, M. Jayaraman, P. C. Ewbank, D. L. Anderson and S. Tristram-Nagle, *Synth. Met.*, 1993, **55**, 1198–1203.
- 6 R. D. McCullough, R. D. Lowe, M. Jayaraman and D. L. Anderson, *J. Org. Chem.*, 1993, 904–912.
- 7 E. E. Sheina, J. Liu, M. C. Iovu, D. W. Laird and R. D. McCullough, *Macromolecules*, 2004, **37**, 3526–3528.
- 8 S. A. Chen and C. S. Liao, *Macromolecules*, 1993, **26**, 2810–2816.
- 9 T. A. Chen and R. D. Rieke, *J. Am. Chem. Soc.*, 1992, **114**, 10087–10088.
- 10 T.-A. Chen, X. Wu and R. D. Rieke, *J. Am. Chem. Soc.*, 1995, **117**, 233–244.
- 11 R. S. Loewe, P. C. Ewbank, J. Liu, L. Zhai and R. D. McCullough, *Macromolecules*, 2001, **34**, 4324–4333.
- 12 R. S. Loewe, S. M. Khersonsky and R. D. McCullough, *Adv. Mater.*, 1999, **11**, 250–253.
- 13 A. Yokoyama, R. Miyakoshi and T. Yokozawa, *Macromolecules*, 2004, **37**, 1169–1171.
- 14 M. C. Iovu, E. E. Sheina, R. R. Gil and R. D. McCullough, *Macromolecules*, 2005, **38**, 8649–8656.
- 15 M. Jeffries-El, G. Sauve and R. D. McCullough, *Adv. Mater.*, 2004, 1017–1019.
- 16 M. Jeffries-El, G. Sauve and R. D. McCullough, *Macromolecules*, 2005, **38**, 10346–10352.
- 17 R. Miyakoshi, A. Yokoyama and T. Yokozawa, *Macromol. Rapid Commun.*, 2004, **25**, 1663–1666.
- 18 T. Beryozkina, V. Senkovskyy, E. Kaul and A. Kiriy, *Macromolecules*, 2008, **41**, 7817–7823.
- 19 N. Doubina, M. Stoddard, H. A. Bronstein, A. K. Y. Jen and C. K. Luscombe, *Macromol. Chem. Phys.*, 2009, **210**, 1966–1972.
- 20 N. Doubina, A. Ho, A. K. Y. Jen and C. K. Luscombe, *Macromolecules*, 2009, **42**, 7670–7677.
- 21 N. Doubina, S. A. Paniagua, A. V. Soldatova, A. K. Y. Jen, S. R. Marder and C. K. Luscombe, *Macromolecules*, 2011, **44**, 512–520.
- 22 H. A. Bronstein and C. K. Luscombe, *J. Am. Chem. Soc.*, 2009, **131**, 12894–12895.
- 23 N. Marshall, S. K. Sontag and J. Locklin, *Chem. Commun.*, 2011, **47**, 5681–5689.
- 24 V. Senkovskyy, N. Khanduyeva, H. Komber, U. Oertel, M. Stamm, D. Kuckling and A. Kiriy, *J. Am. Chem. Soc.*, 2007, **129**, 6626–6632.
- 25 V. Senkovskyy, M. Sommer, R. Tkachov, H. Komber, W. T. S. Huck and A. Kiriy, *Macromolecules*, 2010, **43**, 10157–10161.
- 26 R. Tkachov, V. Senkovskyy, H. Komber and A. Kiriy, *Macromolecules*, 2011, **44**, 2006–2015.
- 27 R. Tkachov, V. Senkovskyy, H. Komber, J.-U. Sommer and A. Kiriy, *J. Am. Chem. Soc.*, 2010, **132**, 7803–7810.
- 28 E. L. Lanni and A. J. McNeil, *J. Am. Chem. Soc.*, 2009, **131**, 16573–16579.
- 29 E. L. Lanni and A. J. McNeil, *Macromolecules*, 2010, **43**, 8039–8044.
- 30 J. R. Locke and A. J. McNeil, *Macromolecules*, 2010, **43**, 8709–8710.
- 31 R. Saha, M. A. Qaium, D. Debnath, M. Younus, N. Chawdhury, N. Sultana, G. Kociok-Koehn, L.-I. Ooi, P. R. Raithby and M. Kijima, *Dalton Trans.*, 2005, 2760–2765.
- 32 M. J. Frisch, G. W. Trucks, H. B. Schlegel, G. E. Scuseria, M. A. Robb, J. R. Cheeseman, G. Scalmani, V. Barone, B. Mennucci, G. A. Petersson, H. Nakatsuji, M. Caricato, X. Li, H. P. Hratchian, A. F. Izmaylov, J. Bloino, G. Zheng, J. L. Sonnenberg, J. L. Hada, M. Ehara, K. Toyota, R. Fukuda, J. Hasegawa, M. Ishida, T. Nakajima, Y. Honda, O. Kitao, H. Nakai, T. Vreven, J. Montgomery, J. A. Montgomery, J. E. Peralta, F. Ogliaro, M. Bearpark, J. J. Heyd, E. Brothers, K. N. Kudin, V. N. Staroverov, T. Keith, R. Kobayashi, J. Normand, K. Raghavachari, A. Rendell, J. C. Burant, S. S. Iyengar, J. Tomasi, M. Cossi, N. Rega, J. M. Millam, M. Klene, J. E. Knox, J. B. Cross, V. Bakken, C. Adamo, J. Jaramillo, R. Gomperts, R. E. Stratmann, O. Yazyev, A. J. Austin, R. Cammi, C. Pomelli, J. W. Ochterski, R. L. Martin, K. Morokuma, V. G. Zakrzewski, G. A. Voth, P. Salvador, J. J. Dannenberg, S. Dapprich, A. D. Daniels, O. Farkas, J. B. Foresman, J. V. Ortiz, J. Cioslowski and D. J. Fox, in *Gaussian 09, Revision B.01*, Gaussian Inc., Wallingford, CT, 2010.
- 33 Y. Zhao and D. G. Truhlar, *Theor. Chem. Acc.*, 2008, **120**, 215–241.
- 34 P. J. Hay and W. R. Wadt, *J. Chem. Phys.*, 1985, **82**, 270–283.
- 35 L. E. Roy, P. J. Hay and R. L. Martin, *J. Chem. Theory Comput.*, 2008, **4**, 1029–1031.
- 36 W. J. Hehre, R. Ditchfield and J. A. Pople, *J. Chem. Phys.*, 1972, **56**, 2257–2261.
- 37 Y. Zhao, B. J. Lynch and D. G. Truhlar, *J. Phys. Chem. A*, 2004, **108**, 2715–2719.
- 38 K. Tamao, K. Sumitani and M. Kumada, *J. Am. Chem. Soc.*, 1972, **94**, 4374–4376.



- 39 R. J. P. Corriu and J. P. Masse, *J. Chem. Soc., Chem. Commun.*, 1972, 144.
- 40 M. Kumada, *Pure Appl. Chem.*, 1980, **52**, 669–679.
- 41 E. Negishi, *Acc. Chem. Res.*, 1982, **15**, 340–348.
- 42 E. Negishi, T. Takahashi, S. Baba, H. D. E. Van and N. Okukado, *J. Am. Chem. Soc.*, 1987, **109**, 2393–2401.
- 43 F. Ozawa, T. Hidaka, T. Yamamoto and A. Yamamoto, *J. Organomet. Chem.*, 1987, **330**, 253–263.
- 44 A. Yamamoto, T. Yamamoto and F. Ozawa, *Pure Appl. Chem.*, 1985, **57**, 1799–1808.
- 45 T. Yamamoto, S. Wakabayashi and K. Osakada, *J. Organomet. Chem.*, 1992, **428**, 223–237.

